Performance Comparison of PRF Schedules for Medium PRF Radar

DALE WILEY

SCOTT PARRY
Royal Australian Air Force

CLIVE ALABASTER

EVAN HUGHES, Member, IEEE
Cranfield University
England

Previous work has shown how evolutionary algorithms (EAs) are an effective tool in optimising the selection of pulse repetition frequency (PRF) values of medium PRF schedules in an airborne fire control radar (FCR) application requiring target data in three PRFs. The optimisation is driven by the requirement to minimise range/Doppler blindness whilst maintaining full decodability. In this paper we detail work in which the optimisation process is applied to design novel short medium PRF schedules requiring target data in just two PRFs. The paper reports on the testing of a variety of near-optimum schedules to compare their blindness, decoding, and ghosting performances. The results show that in many situations, the 2 of N schedules are a practical alternative to conventional 3 of N processing.

Manuscript received February 11, 2005; revised July 5, 2005; released for publication October 31, 2005.

IEEE Log No. T-AES/42/2/876437.

Refereeing of this contribution was handled by E. S. Chornoboy.

Authors' addresses: D. A. Wiley and S. Parry, Royal Australian Air Force; C. Alabaster and E. Hughes, Dept. of Aerospace, Power and Sensors, Cranfield University, Shrivenham, Nr Swindon, Oxfordshire, SN6 8LA, England, E-mail: (c.m.alabaster@cranfield.ac.uk).

0018-9251/06/$17.00 © 2006 IEEE

I. INTRODUCTION

Airborne fire control systems are required to measure both range and velocity of targets in the presence of very high clutter returns from the ground. Unfortunately because of the low grazing angles of the beam with the ground and returns in the antenna sidelobes, the clutter is spread widely in velocity and also exists in most range cells.

Medium pulse repetition frequency (PRF) waveforms offer the best compromise in all aspect detection performance in the presence of clutter and so have become an attractive mode of operation in many of today's military radar systems. The high level of performance demanded from such systems is dependent on the clutter scenario and on the precise values of PRFs chosen, amongst many other factors.

A medium PRF is characterised as being range and velocity ambiguous. Unambiguous range and velocity may be decoded through a comparison of the ambiguous target data received in a minimum number, M, PRFs. Each medium PRF is also characterised by having blind ranges associated with eclipsing losses and overwhelming sidelobe clutter (SLC) and blind velocities associated with the rejection of mainbeam clutter (MBC) and its repetition in the frequency domain. The regions of blindness require that a radar must alternate its operation over several N coherent bursts of PRFs in order to recover sufficient data in the requisite M to resolve ambiguity, in what is known as an M of N schedule.

Decoding true range and velocity places constraints on the selection of precise values of PRF. The decodability of a schedule must be sufficiently robust so as to maintain reliable performance in the presence of multiple targets and when target data is corrupted by measurement tolerances. A potential problem associated with medium PRF operation is the indication of false targets, known as "ghosts," resulting from the correlation of the ambiguous returns of one target with those of another or with noise-generated false alarms. This is also a function of the schedule type (M of N) and precise PRF values but tends to worsen as the number of targets increases.

Previous work by the authors [1, 2] has described the factors affecting the selection of PRF and of the optimisation of the selection of precise values of PRF for an airborne fire control radar (FCR) operating 3 of 8 or 3 of 9 type schedules using evolutionary algorithms (EAs). This work sought to produce schedules which met the requirements of decodability, avoided blind velocities, minimised ghosting, and which were optimised for minimal blindness whilst adhering to system constraints governing maximum, minimum, and mean PRF values.

This paper details the design of novel shorter schedules ($N < 8$) that require target data in only two ($M = 2$) PRFs and is one of the key developments

Authorized licensed use limited to: Cranfield University. Downloaded on November 24, 2009 at 08:17 from IEEE Xplore. Restrictions apply.

of using an evolutionary algorithm to automate the set generation process. The ability to generate fully decodable 2 of N schedules has led to comparisons between 2 of N schedules with the more traditional 3 of N schedules using a model of an airborne FCR to assess the blind zone performances of each. On the whole, the comparisons favour the 2 of N schedules. However, one of the concerns that 2 of N schedules raises is its likelihood of declaring ghost targets in preference to the decoding of the true ranges/velocities of targets, especially as the number of false alarms in any beam position increases. This has therefore led to the formulation of a strategy for decoding true range and velocity whilst minimising the incidence of ghost targets. The decoding and ghosting performance of a variety of near-optimum 3 of N and 2 of N schedules has been compared using the new target extraction algorithm.

Section II discusses some of the key features of medium PRF operation. The section lists the factors affecting the choice of PRF and discusses decodability in greater depth. The section also introduces the concept of 2 of N schedules and discusses the ghosting problem. Section III deals with the methods to optimise the selection of PRFs of a variety of schedule types (M of N) for minimal blindness. The section describes the radar and clutter modelling which are used to assess the quality of each potential solution generated by an EA and hence to drive the optimisation procedure. Section IV describes the work to investigate the decodability and ghosting performance of four near-optimum schedules having minimal blindness. Section V presents the results of the blind zone optimisation and compares the performance of several schedule types. This section also discusses the outcome of the study into the decodability and ghosting performance of some of the near-optimum schedules. Finally, Section VI draws some conclusions; primarily that 2 of N schedules offer superior blind zone performance than 3 of N schedules and incur only marginal degradations in ghosting.

II. MEDIUM PRF OPERATION

A. Factors Affecting PRF

The PRFs of a medium PRF schedule must be selected subject to the following constraints and are described in more detail in [1] and [2].

1) *Decodability*: All combinations of M from N must allow true range and Doppler to be decoded.

2) *Blindness*: The blind ranges and velocities of individual PRFs must be sufficiently dispersed so as to maintain target visibility over the range/Doppler detection space of the radar in as many PRFs as possible.

3) *Blind Velocities*: Blindness over all ranges at particular velocities due to the alignment of the MBC rejection notches (and multiples thereof) in too many PRFs must not be allowed to exist.

4) *Ghosting*: The likelihood of ambiguous returns from one target correlating with those of another target or with a noise-generated false alarm should be minimised.

5) *Maximum PRF*: The upper limit is usually governed by the maximum transmitter duty cycle allowable and also through considerations of the repetition of SLC in the time domain. Also, when combined with the fast Fourier transform (FFT) size, the maximum frequency bin width may be limited by the required velocity resolution.

6) *Minimum PRF*: The lower limit is governed by the consideration that the MBC rejection should not exceed more than 50% of the Doppler band in order to maintain adequate target visibility.

7) *Mean PRF*: The mean value of the N PRFs must be constrained so as to permit the transmission of the entire schedule within the beam dwell time on target.

8) *FFT size*, or alternatively, filter bank size and bin width.

Ideally, PRF selection should be made with due regard to all the above factors. Several of these factors are fundamental to the present work and so are discussed in greater detail in the following paragraphs.

B. Decodability Constraints

Two of the most popular methods of decoding true range and Doppler are the Chinese remainder theorem (CRT) and the coincidence algorithm (CA). The CRT is dismissed here as it constrains the pulse repetition interval (PRI) to be an integer number of range cells and that the number of range cells in every combination of M from N PRI be coprime. These two conditions constrain the PRI unduly. The only decodability constraints enforced by the CA (also required by the CRT) require that (1) and (2) be satisfied for all combinations of M PRFs from the total N, where LCM is the lowest common multiple, $R_{\max}$ is the maximum range, and $D_{\max}$ is the maximum Doppler bandwidth. For example in a 3 of 8 scheme there will be ${}_8C_3 = 56$ inequalities for both range and Doppler giving 112 decodability constraints in total whereas this reduces to a total of 56 for a 2 of 8 scheme

$$\mathrm{LCM}(\mathrm{PRI}_1, \mathrm{PRI}_2, \ldots, \mathrm{PRI}_M) \geq \frac{2R_{\max}}{c}, \qquad \forall \quad {}_NC_M \tag{1}$$

$$\mathrm{LCM}(\mathrm{PRF}_1, \mathrm{PRF}_2, \ldots, \mathrm{PRF}_M) \geq D_{\max}, \qquad \forall \quad {}_NC_M. \tag{2}$$

Authorized licensed use limited to: Cranfield University. Downloaded on November 24, 2009 at 08:17 from IEEE Xplore. Restrictions apply.

Low PRF operation with $M = 1$ satisfies (1) but not (2), whereas high PRF operation with $M = 1$ satisfies (2) but not (1). For modest values of R_{max} and D_{max}, (1) and (2) may be satisfied with $M = 1$, for example battlefield surveillance radar. In the general case $M > 1$ is required.

C. 2 of N versus 3 of N

The minimum number of PRFs in which target data is required in order to resolve range and Doppler ambiguities is, strictly, two. 2 of N schedules require PRFs for which every combination of 2 from N satisfies (1) and (2). A very fine PRI resolution results in a large number of PRIs/PRFs between the maximum and minimum limits and makes the decodability requirements of (1) and (2) easier to satisfy. Relatively coarse PRI resolution of one range cell, which is typical of many current systems, may prevent 2 of N schedules satisfying (1) and (2) and so data is required in a third PRF. This study assumes PRI resolution of 10 ns and so 2 of N schedules are viable.

An initial study to optimise the selection of 2 of N schedules has been conducted and these schedules have been compared with each other and with 3 of N schedules [3]. This work concluded that there were several important ramifications of 2 of N schedules. Since if data is required in only two PRFs, as opposed to three, the total number of PRFs in the schedule that is required, N, may be reduced. Furthermore, range/Doppler blindness is reduced since the radar is now considered blind in regions where there is visibility in fewer than two PRFs (as opposed to three) or detection may be considered marginal when there is visibility in exactly two PRFs. A shorter overall schedule (reduced N) relaxes the constraint on the mean PRI or, alternatively, permits a faster scan rate. The optimisation of the selection of shorter schedules runs more quickly than that for longer schedules and is in keeping with a drive towards dynamic optimisation: decodability of 2 of N schedules can be assessed far more quickly than for 3 of N systems. The one potential danger associated with 2 of N schedules was initially thought to be the greater likelihood of ghost targets, especially as the number of false alarms increases, since target correlation is required in only two PRFs as opposed to three. The selection of M and N will also influence the detection performance of the radar and this is described in [4].

D. Ghosting

In the case of airborne FCR applications, the ghosting performance of 3 of N and 2 of N schedules are considered. 2 of N schedules are likely to report more self-ghosting targets (the correlation of the ambiguous return of one target with that of another target) and noise ghosts (the correlation of the ambiguous return of one target with a noise-generated false alarm) since coincident threshold crossings are required in only two PRFs (as opposed to three). Any target detection appears as a lattice of detection points in range/Doppler detection space due to its repetition in the time and Doppler domains. For a target observed in several PRFs one would observe several such lattices, one for each PRF, with the spacing between points in the time and Doppler domains differing depending on the PRI/PRF. The lattices coincide at the true target range/Doppler, as illustrated in Fig. 1, and therefore the regions of lattice coincidence are the basis for decoding the ambiguities. Measurement error corrupts the range/Doppler coordinates of the lattice points, whilst target smear extends the coordinates over a range of values. In this way it is possible that the detection points at the true target coordinates do not coincide precisely but are merely closely grouped clusters. It also becomes possible that other clusters coalesce in other regions of the range/Doppler detection space and resolving the ambiguities is no longer possible, as illustrated in Fig. 2. Fig. 2 depicts the observation of two targets in six PRFs. The boxes indicate the true locations of the two targets since they encompass a cluster of six detection points. However, there are numerous clusters of fewer detection points which could also be taken for targets. These smaller clusters are typical of ghost targets. This illustrates the problem that the decodability of the schedule is not sufficiently robust to range/Doppler tolerances. The robustness of the decodability of a schedule has been depicted using skyline diagrams in the past [5]. In generating the PRF schedules used in this work a margin for decodability is allowed. No multiples of any two (three) PRIs are allowed to align to within 0.7 μs of each other for 2 (3) of N schedules. In this study, the range cell width = compressed pulse width = 0.5 μs;

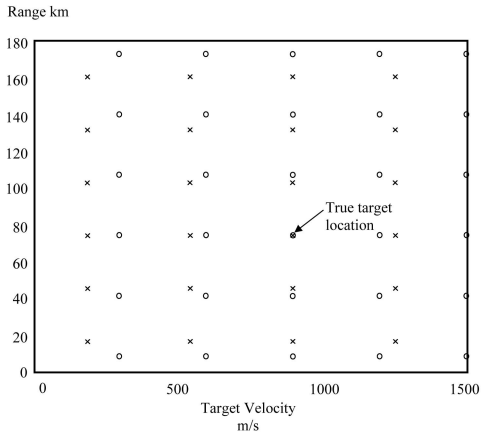


Fig. 1. Lattices of detection points for one target observed in 2 PRFs (x = target detections in PRF1, o = target detections in PRF2).

Authorized licensed use limited to: Cranfield University. Downloaded on November 24, 2009 at 08:17 from IEEE Xplore. Restrictions apply.

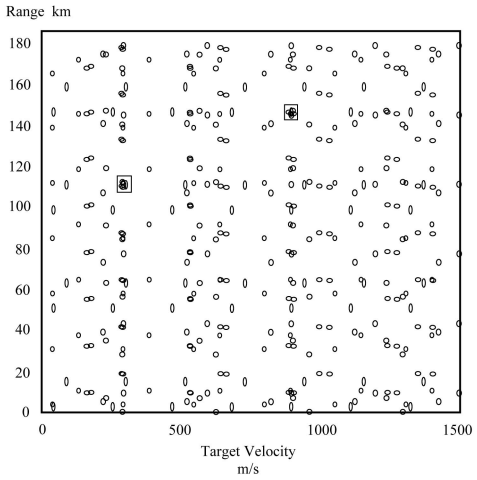


Fig. 2. Clusters of real and ghost targets (two targets observed in six PRFs).

the extra 0.2 μs being the decodability margin. If this margin is increased, it becomes less simple for the EA to find allowable PRF schedules and the blind zone performance of each solution it does find is degraded.

When the lattice points of several targets are displayed on the range/Doppler detection space there becomes a greater likelihood of obtaining false clusters, and so ghost targets, as the number of targets increases. Ironically, the improved blind zone performance of 2 of N schedules compounds the problem slightly, since more detection points will be visible. Therefore, as M is reduced, both the probability of detection and the probability of false alarms increase. The aim is to identify genuine clusters within limits of range/Doppler space and discount the false ones.

III. OPTIMISATION FOR MINIMAL BLINDNESS

A. Optimisation Process

Fig. 3 illustrates the optimisation process that has been employed in the selection of PRFs. The optimisation process is driven by an EA with an optimisation goal of achieving minimal range/Doppler blindness. The EA maintains a population of trial PRF schedules whose values are refined on each iteration of the loop process (generation) along the lines of Darwinian theories of evolution and survival of the fittest [6]. Each trial set is passed to the radar model and the genetic description is decoded to PRF values. This decoding stage employs a variety of checks to ensure that the schedule is decodable, does not incur any blind velocities, enforces a margin to minimise the risk of ghosting and is within the limits of maximum, minimum, and mean PRF, as dictated by the radar model. The PRFs are passed to the radar and clutter models. The clutter model returns the

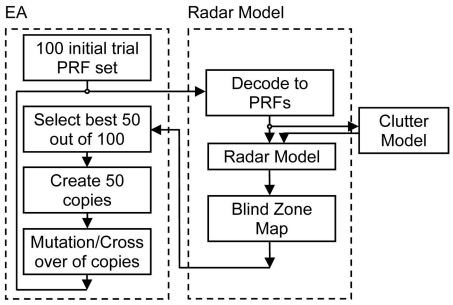


Fig. 3. The optimisation process.

clutter map for each PRF which is also passed to the radar model. The radar model is based on an airborne FCR and accepts the trial PRF schedule and clutter maps. The model then generates a blind zone map and quantifies the area of the range/Doppler detection space which is visible in fewer than $M + 1$ PRFs. The map represents the area which is blind to the radar (visibility in fewer than M PRFs) or where detection is marginal (visible in exactly M PRFs) and is used as a measure of the quality of the trial schedule. This metric is passed back to the EA as the objective value of the trial solution.

The EA applies rules of cross-over and mutation to produce the next generation of trial solutions. These rules favour the retention of good solutions from previous generations but also allow the exploration of the entire search space.

EAs are powerful optimisation techniques which have been successfully employed in a variety of combinatorial problems. They are particularly adept at finding near-optimum solutions very quickly when the number of possible combinations precludes an exhaustive search. It is worth noting that any EA will converge to a solution, however, the efficiency of its convergence and the quality of the solution depend upon the tuning of the algorithm (e.g., population, cross-over, and mutation rates). The EA used here maintains a population of 100, selects the best 50 on each generation and applies cross-over and mutation to generate a further 50 trial solutions. Real valued intermediate cross-over is applied with a probability of cross-over set at 70% and mutation is applied with a zero mean Gaussian distribution; convergence being forced by reducing σ_n of the Gaussian distribution (initially equal to one) by 0.9 on each generation. There exists, as yet, no mathematical description of the performance of an EA. Furthermore, since the number of possibilities in the current problem is so vast, an exhaustive search of all such possibilities is not possible and there can be no confirmation that any particular solution is indeed the global optimum. Hence solutions identified in this work are termed near optimum. In Section V we present results of the EA optimising the selection of 3 of 8, 3 of 9, 2 of 8, 2 of 7, 2 of 6, and 2 of 5 type schedules.

Authorized licensed use limited to: Cranfield University. Downloaded on November 24, 2009 at 08:17 from IEEE Xplore. Restrictions apply.

TABLE I
Radar Model Parameters

Parameters	Value
Carrier frequency	10 GHz
Max & Min PRI	150 to 35 μs
PRI resolution	10 ns (11501 PRIs)
Transmitted pulse width	7 μs
Compressed pulse width	0.5 μs
Compression ratio	14 (linear FM Chirp)
FFT size	64 point
Range resolution	75 m
Blind range due to eclipsing	15 range cells
Duty cycle	Variable (0.2 peak)
Ambiguity resolution	Coincidence algorithm
Beamwidth	3.9°
Scan rate	60°/s
Target illumination time	65 ms
MBC/GMT rejection bandwidth	±1.67 kHz (25 m/s)
Maximum target Doppler	±100 kHz (1500 m/s)
Maximum detection range	185.2 km (100 nmi)
Target radar cross-section	5 m^2
Platform altitude	5000 m
Platform velocity	250 m/s
Antenna depression angle	6°

B. Radar Model

A radar model based on an airborne FCR type was derived to trial the fitness of PRF sets, details of which are summarised in Table I. Note that decodability is required out to a range R_{max} = 185 km (100 nmi) and to a Doppler D_{max} = 100 kHz (velocity = 1500 m/s or Mach 5). Eclipsing is applied throughout the transmitted pulse (7.0 μs) plus the first range cell into the receiver period. Thus range blindness extends to 7.5 μs after the leading edge of the transmitted pulse. The model also allows a 1.7 ms changeover time between PRFs. MBC rejection is applied over a band ±1.67 kHz. Note also that the PRI resolution of 10 ns permits 11501 possible values within the allowable range of 35 to 150 μs.

C. Clutter Modelling

It is assumed that the radar is flown at an altitude of 5000 metres over a surface with a backscatter coefficient of 0.01 m^2/m^2. The antenna has a beamwidth of 3.9° and a constant sidelobe level of −30 dB below the mainbeam. It is further assumed to be directed along a 6° depression angle and that platform motion compensation (PMC) is applied to offset the Doppler of the platform velocity resolved along the antenna boresight to zero Hz.

The clutter model returns a clutter map calculated for each PRF within all trial schedules. A radar target of 5 m^2 is assumed and any point in the range/Doppler detection space having a signal-to-clutter ratio (SCR) < 1 is considered blind. Two different approaches have been tried in order to reduce the processing overhead of the clutter map. The first approach involved calculating the map over a set of widely spread PRFs and then interpolating between the known model instances. Unfortunately, the interpolation process can be time consuming as the number of range cells is different in each PRI. The second approach is to use an approximation for the clutter profile only.

To approximate the clutter profile quickly, the return is calculated for a coarse grid, starting directly below the platform and extending out for two ambiguities in range and Doppler. The beamshape is approximated as constant gain over the beamwidth and then a plateau at the sidelobe level. The coarse approximation and limited investigation of the ambiguities results in approximately 10% error in the prediction compared with using an accurate beam pattern and finely sampled data, wrapped from the entire visibility envelope. The approximation can be performed in typically 3 orders of magnitude faster. As the clutter is modelled as a flat homogenous field, and the backscatter coefficient is only an estimate, the 10% error is well within the modelling error tolerance to be expected when compared with the real scenario.

In a practical radar using dynamic optimisation of the PRF set, the effects of clutter would be assessed based on a combination of approximate models and real clutter measurements from the observed scene.

D. PRF Checks

The PRF selection process maintains a list of all possible PRIs (11501 in the example here). When genetic data is decoded to PRI values a number of checks are enforced at appropriate stages when building up a schedule. These checks ensure that incompatible PRIs are pruned from the list of PRIs and so are not available for future selection.

For a 2 of N schedule, the first PRI is chosen by decoding the first parameter of the genetic description into a valid PRI. For example, for a 2 of 7 system the genetic description consists of seven real-valued numbers in the range $(0, 1]$. The first PRI is found by multiplying the first of the values by the number of available PRIs (11501 to start with) to create an index value. The PRI that lies at the calculated index is chosen, and then removed from the list (leaving 11500 PRIs). All PRIs that are not decodable with the first PRI are removed from the list. The second parameter of the genetic description is then used to calculate an index from the remaining set and the PRI chosen. All PRIs that are not decodable with the second PRI are also removed from the list.

The first checks ensure that the decodability requirements of (1) and (2) are met for all combinations of M from N and that the decodability margin of 0.7 μs is applied (Section IID) to minimise the risk of ghosting. As each PRI is chosen, PRI

Authorized licensed use limited to: Cranfield University. Downloaded on November 24, 2009 at 08:17 from IEEE Xplore. Restrictions apply.

combinations resulting in blind velocities are also rejected. A running check is maintained on the mean PRI which may cap the maximum value allowable for the last few PRIs selected for a schedule should the mean value of previous selections approach the limit. In this way, every schedule is guaranteed to be decodable, be free of blind velocities and adhere to the limits of maximum, minimum, and mean PRF values.

In order to remove invalid PRI combinations quickly, a table can be precalculated that, for each PRI, stores all the PRIs that are not decodable. Thus PRI values that are not decodable can be removed in $O(n.\log_2(n))$ time from the list of available PRIs. As the PRI set reduces, the processing speed also improves. With 3 of N systems, the lookup table is not applicable as all triplets of PRIs must be decodable, rather than all pairs. Fast methods have been developed for systems other than 2 of N but they are slower than the lookup table method.

IV. GHOSTING PERFORMANCE

A. Introduction

The work to optimise the selection of schedules for minimal blindness identified the following near-optimum schedules:

Best 2 of 6 PRIs = 64.04, 74.53, 83.03, 92.07, 100.75, 118.80 μs

Best 2 of 7 PRIs = 73.55, 81.03, 89.76, 99.42, 109.50, 116.46, 125.17 μs

Best 2 of 8 PRIs = 78.92, 81.56, 86.66, 90.46, 99.81, 111.81, 117.09, 128.56 μs

Best 3 of 8 PRIs = 63.11, 69.97, 77.07, 81.31, 90.06, 99.90, 109.75, 119.00 μs

Each of the above schedules has been trialled with the input of multiple targets and an algorithm developed to recognise genuine clusters of detections in each PRF of the schedule from false ones (ghost targets). Two types of multiple target scenarios have been used; the first places between one and five targets at random values of range and Doppler and the second places 4, 6, 8, or 10 targets at 150 m range intervals each with the same Doppler. The former gives a random placement of targets, which is perhaps an unlikely situation in reality whereas the latter represents a close formation, whose range/Doppler centroid is randomly placed on each trial, and is a more likely occurrence. Zero, one or two noise-generated false alarms of random range/Doppler may also be added. A small random variation on target range/Doppler is also imparted over successive PRFs to represent random measurement error and has the effect of spreading the clusters slightly.

B. Target Extraction Algorithm

The algorithm considers the base targets initially, i.e., target detection points within the first unambiguous range and Doppler intervals, and repeats these detection points into the lattices of Fig. 1 by the addition of multiples of the PRI in range and multiples of the PRF in Doppler. Clusters are then formed through the proximity of detection points in different PRFs. The algorithm is based on the concept that genuine targets are characterised by clusters having a large number of detection points, i.e., visible in a large number of PRFs, in a small region of range/Doppler space, whereas ghost targets are more likely to be observed in a few PRFs. It also discounts any clusters containing detection points already attributed to the clusters considered genuine. Therefore, potential ghost target clusters containing the detections of genuine targets which are repeated in the time and frequency domains are dismissed. The target extraction algorithm progresses in the following stages:

1) Expansion of base targets together with an offset made to allow for the range walk of high Doppler shifted targets.
2) Target detection points are sorted in ascending range order.
3) Closely spaced targets are formed into pairs.
4) Closely spaced pairs are formed into clusters.
5) Clusters are checked and possibly subdivided if they contain more than one target detection in any one PRF. In this way, large clusters corresponding to several closely spaced targets generate subclusters; one for each target.
6) Clusters and subclusters are ranked in order of the number of detection points.
7) The process continues by declaring the cluster or subcluster having the greatest number of detection points to be a real target and tags the detection points and their repetition in the time and Doppler domains as having already been declared, potentially reducing the size of some other clusters.
8) The algorithm progresses from largest to smallest clusters and either declaring them as real targets and tagging their detection points or dismissing them as ghosts.

The proximity of detection points which form pairs and hence clusters is an important variable in the success of the algorithm. Rectangles in range/Doppler space of the following dimensions have been trialled: 80 Hz $\times$ 0.6 μs, 50 Hz $\times$ 0.6 μs, 40 Hz $\times$ 0.3 μs, and 25 Hz $\times$ 0.3 μs. These rectangles are based on the range and Doppler resolution and define the dimensions of the maximum allowable cluster sizes.

Authorized licensed use limited to: Cranfield University. Downloaded on November 24, 2009 at 08:17 from IEEE Xplore. Restrictions apply.

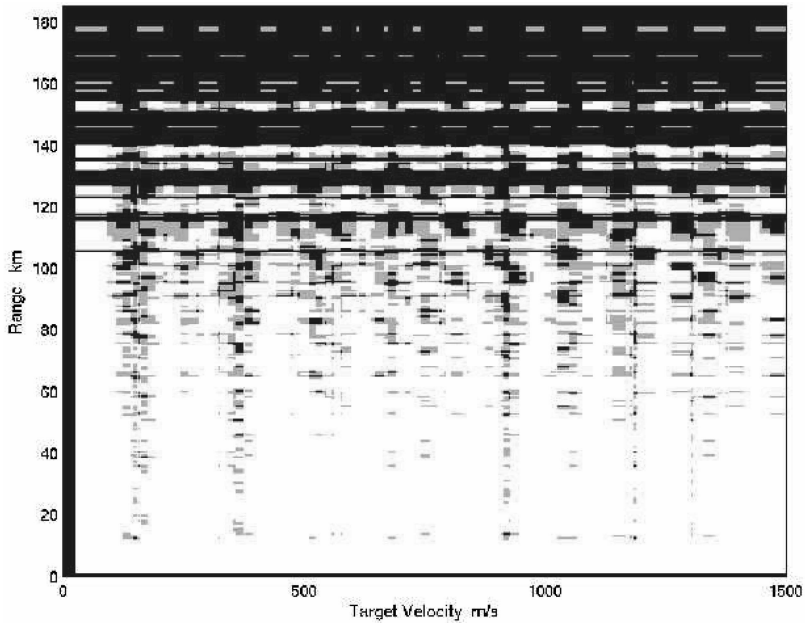


Fig. 4. Blind zone map of best 2 of 8 schedule (black = visibility in fewer than 2 PRFs, grey = visibility in exactly 2 PRFs, white = visibility in more than 2 PRFs).

TABLE II
Test Matrix for Random Targets

PRF Schedules	Number of False Alarms	Cluster Size Hz × μs	Number of Random Targets
2 of 6	0	80 × 0.6	1
2 of 7	1	50 × 0.6	2
2 of 8	2	40 × 0.3	3
3 of 8		25 × 0.3	4
			5

TABLE III
Test Matrix for Close Formation Targets

PRF Schedules	Number of False Alarms	Cluster Size Hz × μs	Number of Close Formation Targets
2 of 6	0	80 × 0.6	4
2 of 7	1	50 × 0.6	6
2 of 8	2	40 × 0.3	8
3 of 8		25 × 0.3	10

C. Testing

The test matrices defined in Tables II and III were derived which explore the various combinations of variables for the randomly distributed targets and close formation targets, respectively. These trials result in 240 combinations for randomly distributed targets and 192 combinations for close formation targets. Five hundred experiments of each combination were run in order to generate statistics on the correctly reported targets, additional targets (i.e., ghosts), genuine targets not reported, and blind targets.

TABLE IV
Blindness Results

M from N	Min %	Max %	Mean %	Median %	σ %
2 from 5	66.10	66.73	66.43	66.44	0.1434
3 from 8	58.37	59.91	59.01	59.02	0.2803
2 from 6	56.35	57.70	57.12	57.18	0.3316
3 from 9	53.74	55.02	54.46	54.51	0.2656
2 from 7	48.90	50.24	49.46	49.54	0.3437
2 from 8	44.13	45.21	44.59	44.57	0.2296

V. RESULTS AND DISCUSSION

A. Blindness

One hundred runs of the optimisation process have been conducted and used to generate the statistics of Table IV. The blindness statistics quoted in Table IV refer to the percentage of the range/Doppler detection space in which targets are visible in fewer than $M + 1$ PRFs and include blindness due to overwhelming SLC, the first blind range and the first blind velocity. Table IV ranks the schedules in order of blindness performance. It is clear that blindness is minimised by reducing M and increasing N, with the former having the most significant effect. Of particular note is the fact that 2 of 6 schedules marginally outperform 3 of 8 schedules. The blind zone map of the best 2 of 8 schedule is plotted in Fig. 4. This has blindness (visibility in fewer than 3 PRFs) extending over 44% of the map, the majority of which is due to overwhelming SLC. The blind zone map of the best 3 of 8 schedule is plotted in Fig. 5. This has blindness (visibility in fewer than 4 PRFs) extending over 58% of the map and is also dominated by high SLC at long ranges.

Authorized licensed use limited to: Cranfield University. Downloaded on November 24, 2009 at 08:17 from IEEE Xplore. Restrictions apply.

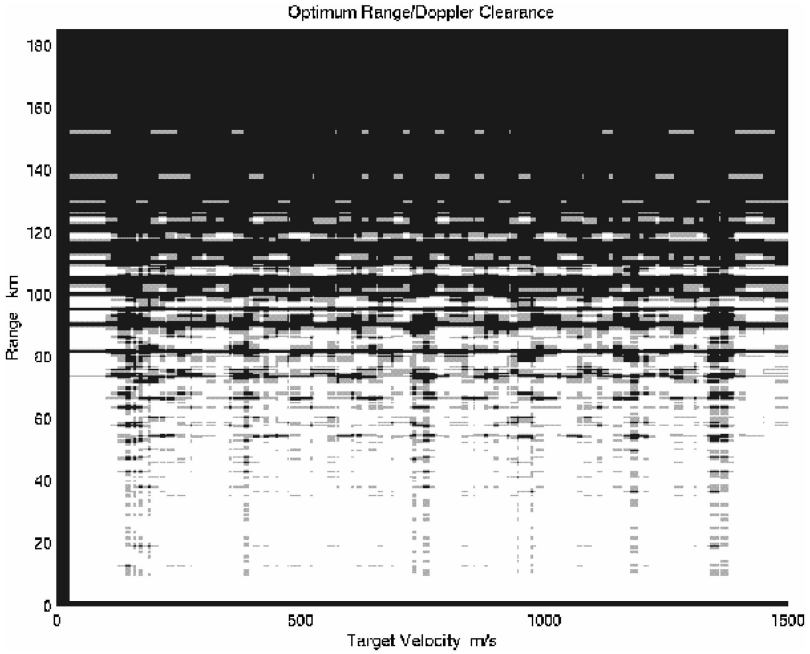


Fig. 5. Blind zone map of best 3 of 8 schedule (black = visibility in fewer than 3 PRFs, grey = visibility in exactly 3 PRFs, white = visibility in more than 3 PRFs).

B. Ghosting

Each schedule is quantified in terms of the correctly reported targets, additional (ghost) targets, targets which remained blind, and targets not reported (but not blind). All statistics are quoted as percentages of the total number of targets. Thus 500 runs of 4 targets give a total of 2000 targets and 20 occurrences of ghosts would therefore be expressed as 1%. The test matrices of Tables II and III define 240 and 192 test combinations for the randomly distributed targets and close formation targets, respectively. Each test has been applied to four near-optimum schedules. This means that 432 tests are made on each schedule, i.e., 1728 tests in total. Of the 1728 tests, four metrics are used to quantify the performance, as described above. Obviously, a massive amount of data is derived from these tests and naturally this has been summarised for this paper.

When one to five random targets were applied approximately 95% of them were correctly reported, irrespective of the schedule, number of false alarms, or of the allowable cluster size. The 2 of 8 schedule was consistently the best and the 2 of 6 and 3 of 8 schedules were the worst being about 2% lower.

Additional ghost targets were generally lower than 0.5% of total applied targets. For ghosting, the 3 of 8 schedule was consistently the best as it reported no additional targets in all the runs without false alarms, and only the occasional ghost was seen with 2 false alarms; there was no consistently worst schedule. There was no significant increase in ghosts when one false alarm was applied over the case of zero false alarms. However, an increase in ghosts to around 1–4% (depending on allowable cluster size) for the 2 of N schedules was seen when 2 false alarms and only one or two targets were applied and was attributable to the correlation of one false alarm with the other. Generally, ghost target percentages increased with increasing allowable cluster size but reduced with increasing number of real targets. This is perhaps surprising but is due to the fact that in identifying several genuine targets, the algorithm tags most of the detection points and in so doing the smaller clusters typical of ghosts are more readily discounted.

About 5% of applied targets remained blind, irrespective of the numbers of false alarms and allowable cluster size. The blindness statistics of each schedule mirrored their blind zone performances, see Table IV; 2 of 8 being best and 3 of 8 being some 2% higher. Generally, fewer than 1% of targets were not reported, the 3 of 8 schedule being the best.

When 4, 6, 8 or 10 targets in a close formation were applied about 95% were correctly reported and is independent of allowable cluster size and numbers of false alarms but reduced with increasing numbers of targets. The 2 of 8 schedule was consistently best and the 2 of 6 worst being about 5% lower. The reduction with increasing target numbers is due to the greater likelihood of ghosts being reported in preference to genuine targets in regions of marginal visibility.

The number of ghosts is somewhat greater for the close formation targets than those of random placement. This is due to the fact that all targets have the same Doppler and so alignment in range only is required to form a ghost. The 2 of 6 schedule reports the highest incidence of ghosts which rises from 1

Authorized licensed use limited to: Cranfield University. Downloaded on November 24, 2009 at 08:17 from IEEE Xplore. Restrictions apply.

TABLE V
Worst Case Ghosting Statistics

PRF Schedule	Worst Case Ghosting	Conditions of Worst Case Ghosting
2 of 6	7.5%	80 Hz × 0.6 μs, 2 false alarms, 10 formation targets
2 of 7	4.0%	50 Hz × 0.6 μs, 2 false alarms, 1 random target
2 of 8	3.0%	50 Hz × 0.6 μs and 80 Hz × 0.6 μs, 2 false alarms, 1 random target
3 of 8	1.3%	80 Hz × 0.6 μs, 1 and 2 false alarms, 8 to 10 formation targets

to 6% as the number of targets increases from 4 to 10. The number of ghosts also rises as the allowable cluster size increases and rises very slightly as the number of false alarms increases. It peaks at a value of around 7.5% for the 2 of 6 schedule (2 false alarms, 10 targets and an allowable cluster size of 80 Hz × 0.6 μs). The 3 of 8 schedule consistently had the best ghosting performance with a peak value of 1.3% under similar conditions. Longer schedules tend to result in fewer ghosts as they give rise to clusters having a greater number of detection points which are more readily identified as targets in preference to the smaller clusters of ghosts. The worst case ghosting statistics and the test conditions under which they were observed are summarised in Table V. The best case ghosting was 0% for all schedules and was obtained under a variety of test conditions. It ought to be borne in mind that the ghosting performance is but one metric used to assess the quality of each schedule and even though it is of key consideration ghosting should not be viewed in isolation of the other metrics, namely, correctly reported targets, targets which remained blind, and targets not reported (but not blind).

The numbers of targets not reported follows the trend in ghosting performance since the reporting of a ghost is usually done in preference to the reporting of a target. Blind target results follow the same pattern as for the random targets which mirror the blind zone performance of each schedule.

It is interesting to note that although 2 of N schedules do result in more ghost clusters than 3 of N schedules, the rules of the target extraction algorithm have succeeded in dismissing the vast majority. Much of this success is due to the system of giving preferential treatment to longer clusters, tagging data associated with targets and dismissing clusters containing previously tagged data. It is also worth noting that the observation of multiple targets in 3 PRFs gives rise to more cross-correlation possibilities than for 2 PRFs and hence 3 of N schedules are naturally more inclined to ghost than 2 of N schedules. For example, if 2 targets are observed in 2 PRFs there are 4 cross-correlation possibilities, two of which correspond to the correct targets and the other two are potential ghosts. Whereas, if 2 targets are observed in 3 PRFs there are 8 cross-correlation possibilities corresponding to the two targets plus 6 potential ghosts. In general, the number of potential ghosts is given by $N_T^{N_{\mathrm{PRF}}} - N_T$ where N_T is the number of targets and N_{PRF} the number of PRFs in which the targets were observed.

VI. CONCLUSIONS

The EA has been successful in optimising the selection of PRF values of various medium PRF schedules for minimal range/Doppler blindness. Repeated runs of the EA identify several near-optimal PRF sets whose blindness differs marginally from each other. These repeats indicate the existence of several similar local optima in the problem space and the ability of the EA to find them. Blindness is minimised in schedules requiring target data in fewer PRFs ($M = 2$) and for longer schedules ($N = 8$). Of the two, the reduction in M is the most significant. Thus the schedule having least blindness is the 2 of 8 which has some 14% less blindness than the 3 of 8 schedule, and an overall higher probability of detection. The most noticeable improvement occurs at ranges around 60 to 150 km, beyond which high SLC levels form the dominant cause of blindness.

The numbers of ghost targets remained very low for the 3 of 8 schedule but were degraded in the 2 of N schedules; the peak worst cases being some 2.3 to 5.8 times higher. The target extraction algorithm was most reliable for the longer schedules. Close formation targets gave rise to more ghosts than targets of random range and Doppler since close formations of identical Doppler only require correlation in range to register as ghosts. Unreported targets were very low in all schedules but tended to follow the trends in the reporting of ghosts. Correctly reported targets were maintained at a high level but were marginally superior for the 2 of 8 schedule. The highest incidence of ghosts (2 of 6, close formation targets) also corresponded to the lowest incidence of correctly reported targets, since ghosts were being declared in preference to correct targets. The numbers of blind targets followed the trend in blind zone performance.

During the course of the ghosting tests it was found that the incidence of ghosts was determined by the inherent inclination of the PRF schedule to cross-correlate target returns and/or noise-generated false alarms together with the margin of the inequality of (1) and (2). This inequality is the margin by which the extent of the unambiguous detection range/Doppler space as defined by the left-hand sides of (1) and (2) exceeds the range/Doppler space of interest as defined by the radar model and therefore by the right-hand sides of (1) and (2). For example,

Authorized licensed use limited to: Cranfield University. Downloaded on November 24, 2009 at 08:17 from IEEE Xplore. Restrictions apply.

the PRI pair of 19 μs and 21 μs have a maximum unambiguous range associated with a delay of 399 μs. If, however, a third PRI of 23 μs is introduced, the overall maximum unambiguous range is extended by a factor of 23 to 9177 μs. The addition of the third PRI/PRF extends the decodable range/Doppler region enormously. 2 of N schedules appear to be less inclined to form ghosts but since the left-hand sides of (1) and (2) are only just greater than the right-hand sides most of these ghosts fall within the range/Doppler space of interest. 3 of N schedules were more inclined to ghost but since the left-hand sides of (1) and (2) are significantly greater than the right hand sides, proportionately fewer ghosts fall within the range/Doppler space of interest. The net result is that 3 of N schedules have somewhat superior ghosting statistics to the 2 of N schedules but in all cases the numbers of ghosts are relatively low.

The performance of the 2 of N schedules and the principles of the optimisation process that yielded such schedules have been illustrated by the example of the particular radar and clutter models used here. The precise PRF values generated are valid for the FCR model parameters considered here and so are of limited general interest. Nevertheless, the general trends in blind zone performance and target extraction/minimisation of ghosts will apply to a wide range of radars. Therefore, we predict confidently that the methods used here and these conclusions are applicable in a general sense.

In summary, each schedule type has areas of relative strength and weakness, however, the best and worst schedules found do not differ appreciably from each other. The original fears regarding the ghosting performance of 2 of N schedules appear to have been unfounded for the proposed target extraction algorithm. This study has shown that 2 of N schedules can be considered viable and even advantageous with respect to the more conventional 3 of N schedules, not only in radar applications such as airborne fire control, but especially those of a modest range/Doppler detection space and limited dwell time. In particular, the detection performance of an optimal 2 of 6 schedule is very similar to that of an optimal 3 of 8 schedule but enjoys the benefits of being a shorter schedule.

REFERENCES

[1] Davies, P. G., and Hughes, E. J.
Medium PRF set selection using evolutionary algorithms.
IEEE Transactions on Aerospace and Electronic Systems, **38**, 3 (July 2002), 933–939.

[2] Alabaster, C. M., Hughes, E. J., and Matthew, J. H.
Medium PRF radar PRF selection using evolutionary algorithms.
IEEE Transactions on Aerospace and Electronic Systems, **39**, 3 (July 2003), 990–1001.

[3] Hughes, E. J., and Alabaster, C. M.
Novel PRF Schedules for medium PRF radar.
In *Proceedings of the Radar 2003 Conference*, Adelaide, S. Australia, September 3–5, 2003.

[4] Wilson, S. L., and Carlson, B. D.
Radar detection in multipath.
IEE Proceedings, Radar, Sonar Navigation, **146**, 1 (Feb. 1999), 45–54.

[5] Kinghorn, A. M., and Williams, N. K.
The decodability of multiple-PRF radar waveforms.
In *Proceedings of IEE Radar 97*, Edinburgh, UK, Oct. 1997, Conference Publication 449.

[6] Zalzala, A. M. S., and Flemming, P. J. (Eds.)
Genetic Algorithms in Engineering Systems.
London: The Institution of Electrical Engineers, 1997.



Flt. Lt. Dale A. Wiley received his B.Eng. degree in electrical engineering from the University of New South Wales, Sydney, Australia, in 1997 and his M.Sc. in military electronic systems engineering from Cranfield University, Shrivenham, England, in 2003.

From 1998 to 1999 he was posted to the Aircraft Research and Development Unit and worked on Telemetry post-processing software. He was posted to the Electronic Warfare Squadron in 2000 where he worked on reprogramming radar warning receivers and RF jammer threat libraries for 2 years. He is currently working for the Joint Electronic Warfare Operational Support Unit developing RF and EO countermeasures for the F-111 and F/A-18.

Flt. Lt. Wiley is a member of the Institute of Engineers Australia.

Authorized licensed use limited to: Cranfield University. Downloaded on November 24, 2009 at 08:17 from IEEE Xplore. Restrictions apply.



Sqn. Ldr. Scott M. Parry received his B.Eng. degree in electrical engineering from the University of New South Wales, Australia in 1996. He completed his M.Sc. degree in military communication systems engineering from the Cranfield University at the Royral Military College of Science, Cranfield, England.

He has been employed by the Royal Australian Air Force (RAAF) since 1996 in roles ranging from software requirements and certification, aircraft systems engineering, electronic warfare, and aircraft maintenance management. He is currently the project engineering manager for the RAAF F/A-18 Electronic Warfare Self Protection Suite upgrade.

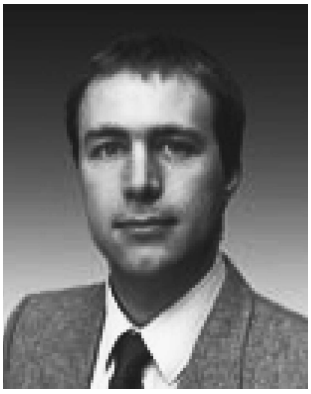
Sqn. Ldr. Parry is a member of Institute of Engineers Australia.



Clive M. Alabaster received his B.Sc. degree in physics with microelectronics from University College Swansea, Wales, in 1985 and his Ph.D. from Cranfield University, Shrivenham, England, in 2004.

From 1985 to 1992 he worked as a microwave design and development engineer on airborne radar systems with GEC Marconi, Milton Keynes, England. From 1992 to 1998 he worked as a lecturer in radar techniques at Arborfield Garrison, near Reading, England. He joined Cranfield University at the Royal Military College of Science, Shrivenham, in 1998 as a lecturer in the Radar Systems group within the Department of Aerospace, Power and Sensors. His research interests include the optimisation of radar waveforms, radar, dielectric materials, the measurement of permittivity, particularly in the millimetre wave band and the nondestructive testing of composite materials using microwaves/millimetre waves.

Dr. Alabaster is a member of the Institute of Physics and is a Chartered Engineer.



Evan J. Hughes (S'96—A'98—M'99) received his B.Eng. and M.Eng. degrees in electrical and electronic engineering from the University of Bradford, England, in 1993 and 1994, respectively. He received his Ph.D. in 1998 from Cranfield University at the Royal Military College of Science, Shrivenham, England.

From 1993 to 1995 he worked as a design engineer with GEC Marconi, Leicester. He is currently working as a senior lecturer for the Radar Systems group in the Department of Aerospace, Power and Sensors. His primary research interests include noisy multi-objective evolutionary algorithms, swarm guidance, data fusion, artificial neural networks, fuzzy systems, intelligent agents and radar systems.

Dr. Hughes is a member of the IEE and is a Chartered Engineer. He received the prize for best paper at GALESIA '97, Glasgow, UK, won the Evolutionary Checkers Competitions at CEC 2001, Seoul, S. Korea and WCCI 2002, Honolulu, Hawaii, and won the Time Series Prediction Competition at WCCI 2002.

Authorized licensed use limited to: Cranfield University. Downloaded on November 24, 2009 at 08:17 from IEEE Xplore. Restrictions apply.



https://dspace.org/

The Design of medium PRF radar schedules for optimum detectability in diverse clutter scenes

Alabaster, Clive M.; Hughes, Evan J.

2009-04-22T14:28:48Z
IEEE
http://hdl.handle.net/1826/3343

Alabaster CM, Hughes EJ. (2006) The design of medium PRF radar schedules for optimum detectability in diverse clutter scenes. In: 2006 International Waveform Diversity & Design Conference, 22-27 January 2006, Lihue, HI, USA

Downloaded from a DSpace repository. https://dspace.org/